Available online at www.sciencedirect.com
SCIENCE DIRECT
INTERNATIONAL JOURNAL OF MACHINE TOOLS & MANUFACTURE
DESIGN, RESEARCH AND APPLICATION
International Journal of Machine Tools & Manufacture 43 (2003) 1561–1569

Sensitivity analysis of the 3-PRS parallel kinematic spindle platform of a serial-parallel machine tool

Kuang-Chao Fan [a,*], Hai Wang [b], Jun-Wei Zhao [c], Tsan-Hwei Chang [d]

[a] *Department of Mechanical Engineering, National Taiwan University, 1, Sec. 4, Roosevelt Road, Taipei, Taiwan, ROC*
[b] *Department of Mechanical Engineering, Ming-Chi Institute of Technology, Taipei, Taiwan, ROC*
[c] *School of Mechanical Engineering, Jiao Zhou College of Engineering, Henan, China*
[d] *Mechanical Industry Research Laboratory, ITRI, Taichung, Taiwan, ROC*

Received 1 April 2003; accepted 9 July 2003

Abstract

The special configuration of a serial-parallel type machine tool possesses five degrees of freedom and provides more flexibility in NC machining. The parallel spindle platform plays the key role in manipulating three directions of movement. In this study, the inverse kinematics analysis of the platform is derived first. A sensitivity model of the spindle platform subject to the structure parameters is then proposed and analyzed. All the parameters influencing the position and orientation of the spindle platform are discussed based on the sensitivity model and the simulated examples. Critical parameters to the accuracy of the cutter location can then be found, which are the slider position, the strut length, and the tool length.

Keywords: Kinematic analysis; Sensitivity analysis; 3-PRS spindle platform; Serial-parallel machine tool

1. Introduction

To obtain higher accuracy and greater dexterity, machine tool manufacturers are developing parallel type structures for the next generation of machine tools. It is always a goal to pursue an interesting development in the machine tool industry that holds great promise for improving accuracy. Machine tools with their high rigidity and accuracy are ideally suited for precision applications. Parallel manipulator offers a radically different type of machine structure relative to the traditional serial type machines. It is believed that the inherent mechanical structure of the parallel type machines provides high dexterity, stiffness, accuracy and speed compared to the conventional multi-axis structure [1,2].

In the past, many comprehensive studies and works have been made in the area of parallel manipulators. The kinematic behavior of the parallel mechanism with extensible strut has been discussed in many literatures [3–5]. Some reports dealt with the kinematics of three-legged parallel manipulators [6,7]. Most of these articles focused on the discussion of both the analytical and the numerical methods to solve the kinematics of pure-parallel mechanisms [6–8]. Some papers also discussed the accuracy analysis of the Stewart platform manipulators [9–11]. A new type of serial-parallel machine tool has been developed by the Mechanical Laboratory of ITRI in Taiwan. Simulation analysis and experimental tests have shown the necessity of its accuracy enhancement [12–14].

Even though many researches have made contributions to the theory and design of the parallel kinematic mechanism, however, commercial applications of this potential parallel machine have not been widespread yet. The main obstacle to the applications of this kind of machine tool is their unsatisfactory accuracy. Similar to the traditional machine tool, there are several major factors, such as the structural imperfection, the elastic deformation and the thermal deformation, that will degrade the machine accuracy. In order to find out the essential error sources, sensitivity analysis of the spindle platform movement and error identification are neces-

* Corresponding author. Tel.: +02-23620032; fax: +02-23641186.
E-mail address: fan@ccms.ntu.edu.tw (K.-C. Fan).

0890-6955/$ - see front matter
doi:10.1016/S0890-6955(03)00202-5

sary for the purpose of accuracy enhancement of the machine tool.

In this paper, the kinematics model of parallel mechanism is derived in the first part. Sensitivity model of the spindle platform subject to structural and kinematic parameters is then proposed. All parameters influencing the position and orientation of the spindle platform are analytically estimated. Simulated example are given to identify the most critical error sources.

2. Machine tool configuration

The machine tool under investigation is called a serial-parallel type machine tool. The configuration is shown in Fig. 1. It consists of a three-degree-of-freedom spindle platform and a conventional two-degree-of-freedom *X*–*Y* table to form a five-axis structure. The spindle is assembled in the platform, which is connected to three struts of constant length by means of ball joints (or U-joint) that are equally spaced at a nominal angle of 120°. The other end of each strut is connected to a slider with a rotational joint. Each slider can move up and down along the corresponding vertical slideway fixed to a column that is also spaced at nominal 120° angle from one another. The platform, such constructed, has one linear motion in the *Z*-axis and two angular rotations (α and β) in the *X*- and *Y*-axes, respectively. The *X*–*Y* table that supports the workpiece provides the linear motions of the workpiece in two horizontal directions. The features of this configuration are easy to manufacture and control, more accurate and larger workspace, compared to the Stewart platform-based parallel machine tool.

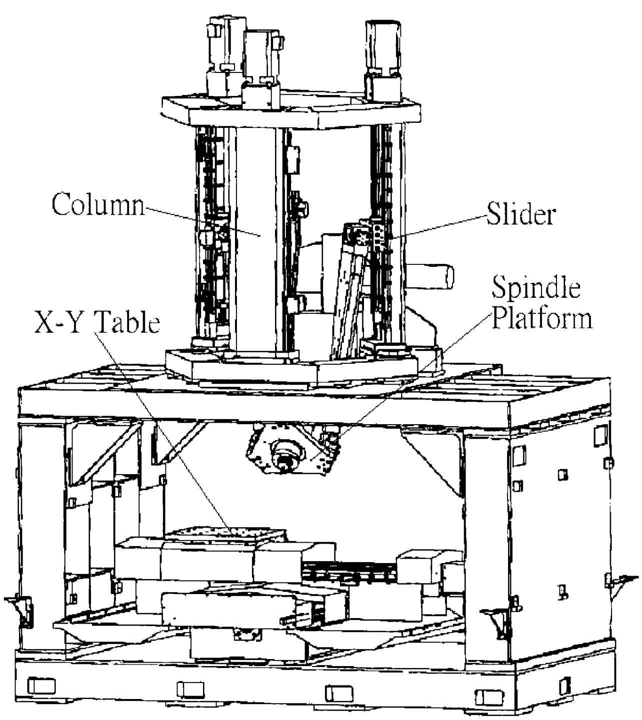

Fig. 1. Structure of the serial-parallel type machine tool.

3. Inverse kinematic analysis

In order to analyze the kinematics of the parallel mechanism, three relative coordinate frames are assigned, as shown in Fig. 2. A static Cartesian coordinate frame *XYZ* is fixed at the base of the machine tool with the *Z*-axis pointing to the vertical direction, the *X*-axis pointing toward B_1, and the *Y*-axis pointing along the B_2B_3 line. The movable Cartesian coordinate frame, $X'Y'Z'$, is fixed at the center of the *X*–*Y* table with the same axes directions as the *XYZ* coordinate frame. The third coordinate frame, *xyz*, is assigned to the tool tip, with the *z*-axis coinciding with the spindle axis. The ball joint b_1 is located in the plane xo_Tz.

Let *R* and *r* be the radii of circles passing through joints R_i and b_i (i = 1–3), respectively. The positions of R_i referenced to the coordinate frame *XYZ* can be expressed by

$$\mathbf{R}_1 = \begin{bmatrix} \frac{3}{2}R & 0 & H_1 \end{bmatrix}^T \mathbf{R}_2 = \begin{bmatrix} 0 & \frac{\sqrt{3}}{2}R & H_2 \end{bmatrix}^T \tag{1}$$

$$\mathbf{R}_3 = \begin{bmatrix} 0 & -\frac{\sqrt{3}}{2}R & H_3 \end{bmatrix}^T$$

where H_i is the height of R_i along the *Z*-axis.

The positions of the ball joints b_i with respect to the coordinate frame *xyz* are

$$\mathbf{b}_1 = [r \;\; 0 \;\; h]^T \mathbf{b}_2 = \begin{bmatrix} -\frac{1}{2}r & \frac{\sqrt{3}}{2}r & h \end{bmatrix}^T \tag{2}$$

$$\mathbf{b}_3 = \begin{bmatrix} -\frac{1}{2}r & -\frac{\sqrt{3}}{2}r & h \end{bmatrix}^T$$

where *h* is the distance from the tool tip o_T to the center of the platform.

The coordinate frame *xyz* with respect to the coordinate frame *XYZ*, can be described by the homogeneous transformation matrix [**T**].

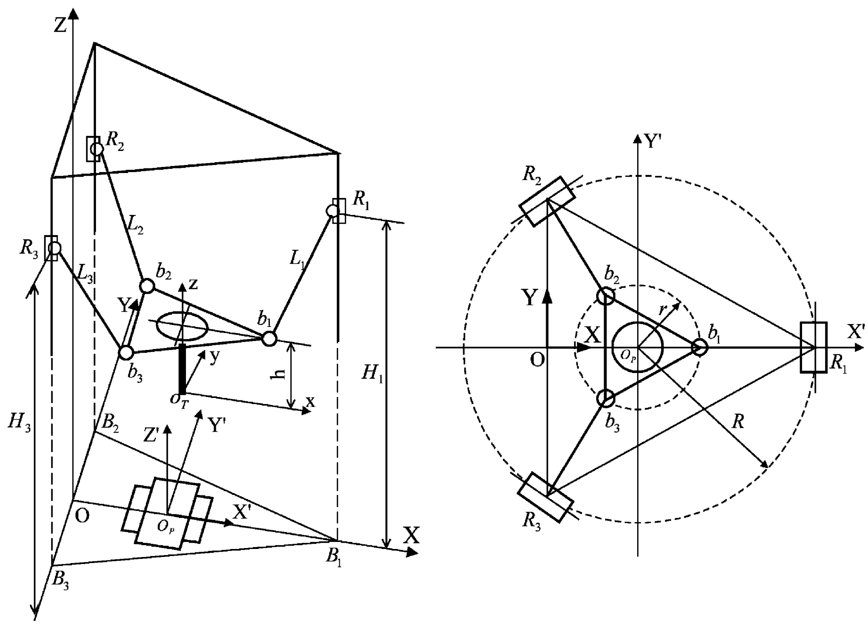

Fig. 2. Schematic diagram of the serial-parallel structure.

$$[\mathbf{T}] = \begin{bmatrix} k_1 & m_1 & n_1 & x_T \\ k_2 & m_2 & n_2 & y_T \\ k_3 & m_3 & n_3 & z_T \\ 0 & 0 & 0 & 1 \end{bmatrix} = \tag{3}$$

$$\begin{bmatrix} C\beta C\gamma & -C\beta S\gamma & S\beta & x_T \\ S\alpha S\beta C\gamma + C\alpha S\gamma & -S\alpha S\beta S\gamma + C\alpha C\gamma & -S\alpha C\beta & y_T \\ -C\alpha S\beta C\gamma + S\alpha S\gamma & C\alpha S\beta S\gamma + S\alpha C\gamma & C\alpha C\beta & z_T \\ 0 & 0 & 0 & 1 \end{bmatrix},$$

where $[x_T\ \ y_T\ \ z_T]^T = {}^o\mathbf{p}$ is the position vector of the origin of the frame xyz (tool tip position), and the orientation unit vectors $\mathbf{k} = [k_1\ \ k_2\ \ k_3]^T$, $\mathbf{m} = [m_1\ \ m_2\ \ m_3]^T$, and $\mathbf{n} = [n_1\ \ n_2\ \ n_3]^T$ are the directional cosines of the axes x, y and z with respect to the coordinate frame XYZ. $S\alpha$, $S\beta$, $S\gamma$, $C\alpha$, $C\beta$ and $C\gamma$ indicate sin α, sin β, sin γ, cos α, cos β and cos γ, respectively. α, β and γ are the rotational angles (also called the Euler angles) of the spindle platform with respect to the X-, Y- and Z-axes, respectively.

The Cartesian position of the ball joints $\mathbf{b}_i$ with respect to the frame XYZ can be expressed by

$$\begin{bmatrix} \mathbf{b}_i \\ 1 \end{bmatrix}_o = \begin{bmatrix} {}^o_{o_T}\mathbf{R} & {}^o\mathbf{p} \\ 0 & 1 \end{bmatrix} \cdot \begin{bmatrix} \mathbf{b}_i \\ 1 \end{bmatrix}_{o_T} = [\mathbf{T}] \cdot \begin{bmatrix} \mathbf{b}_i \\ 1 \end{bmatrix}_{o_T} \quad i = 1,2,3 \tag{4}$$

Substituting those vector forms of Eq. (2) into Eq. (4) yields

$$\begin{bmatrix} \mathbf{b}_1 \\ 1 \end{bmatrix}_o = \begin{bmatrix} X_1 \\ Y_1 \\ Z_1 \\ 1 \end{bmatrix} = \begin{bmatrix} rk_1 + hn_1 + x_T \\ rk_2 + hn_2 + y_T \\ rk_3 + hn_3 + z_T \\ 1 \end{bmatrix} \tag{5}$$

$$\begin{bmatrix} \mathbf{b}_2 \\ 1 \end{bmatrix}_o = \begin{bmatrix} X_2 \\ Y_2 \\ Z_2 \\ 1 \end{bmatrix} = \begin{bmatrix} -\frac{r}{2}k_1 + \frac{\sqrt{3}r}{2}m_1 + hn_1 + x_T \\ -\frac{r}{2}k_2 + \frac{\sqrt{3}r}{2}m_2 + hn_2 + y_T \\ -\frac{r}{2}k_3 + \frac{\sqrt{3}r}{2}m_3 + hn_3 + z_T \\ 1 \end{bmatrix} \tag{6}$$

$$\begin{bmatrix} \mathbf{b}_3 \\ 1 \end{bmatrix}_o = \begin{bmatrix} X_3 \\ Y_3 \\ Z_3 \\ 1 \end{bmatrix} = \begin{bmatrix} -\frac{r}{2}k_1 - \frac{\sqrt{3}r}{2}m_1 + hn_1 + x_T \\ -\frac{r}{2}k_2 - \frac{\sqrt{3}r}{2}m_2 + hn_2 + y_T \\ -\frac{r}{2}k_3 - \frac{\sqrt{3}r}{2}m_3 + hn_3 + z_T \\ 1 \end{bmatrix} \tag{7}$$

Obviously, as each strut is constrained by the corresponding rotational joint and ball joint, strut 1 can only move in the plane Ω_1: $Y = 0$; strut 2 in the plane Ω_2:

$Y = -\sqrt{3}(X - R/2)$; and strut 3 in the plane Ω_3: $Y = \sqrt{3}(Y - R/2)$, as shown in Fig. 3. According to Eqs. (5) and (7), three constraint equations can thus be obtained as

$$rk_2 + hn_2 + y_T = 0 \tag{8}$$

$$-\frac{1}{2}rk_2 + \frac{\sqrt{3}}{2}rm_2 + hn_2 + y_T = -\sqrt{3}\left(-\frac{1}{2}rk_1 + \frac{\sqrt{3}}{2}rm_1 + hn_1 + x_T - \frac{R}{2}\right) \tag{9}$$

$$-\frac{1}{2}rk_2 + \frac{\sqrt{3}}{2}rm_2 + hn_2 + y_T = \sqrt{3}\left(-\frac{1}{2}rk_1 + \frac{\sqrt{3}}{2}rm_1 + hn_1 + x_T - \frac{R}{2}\right) \tag{10}$$

Summing up Eqs. (9) and (10), and then simplified by Eq. (8), it yields

$$m_1 = k_2 \tag{11}$$

Subtracting Eq. (9) from Eq. (10), it yields

$$\frac{r}{2}(k_1 - m_2) - hn_1 + \frac{R}{2} = x_T \tag{12}$$

Substituting m_1 and k_2 from Eqs. (3) and (11), the γ can be obtained as

$$\gamma = f(\alpha,\beta) = -\arctan\left(\frac{\sin\alpha\sin\beta}{\cos\alpha + \cos\beta}\right). \tag{13}$$

Eq. (13) indicates that γ is a function of α and β. Eqs. (12) and (8) indicate that x_T and y_T are both functions of directional cosines. x_T and y_T can further be expressed in terms of the Euler angles as:

$$x_T = \frac{r}{2}(\cos\beta\cos\gamma + \sin\alpha\sin\beta\sin\gamma - \cos\alpha\cos\gamma) - h\sin\beta + \frac{R}{2} \tag{14}$$

$$y_T = h\sin\alpha\cos\beta - r\sin\alpha\sin\beta\cos\gamma - r\cos\alpha\sin\gamma$$

Eqs. (13) and (14) show that if α, β, and z_T are known, x_T and y_T can be determined. The transformation matrix [**T**] can then be obtained by Eq. (3), and the Cartesian position of each ball joint with respect to the frame XYZ can be calculated using Eq. (4). As the strut length l_i is constant, the position component of the rotational joint in the Z-axis can be calculated using the inverse kinematics as

$$H_i = R_{iZ} = \pm\sqrt{l_i^2 - (R_{iX} - b_{iX})^2 - (R_{iY} - b_{iY})^2} + b_{iZ} \quad i = 1,2,3 \tag{15}$$

Eq. (15) has two solutions, but the position of rotational joint is always above the ball joint. Only the positive solution is effective.

The inverse kinematics problem involves the computation of the position of each of the rotational joint (the slider) through the corresponding ball joint if the spindle platform's position and orientations are known.

4. Sensitivity analysis of the spindle platform

On the basis of the machine tool configuration, its structure actually consists of three parallel structural loops. For each loop, a closed form of vector chain of the linkage can be drawn, as shown in Fig. 4. The related equation can be presented in the following vector form.

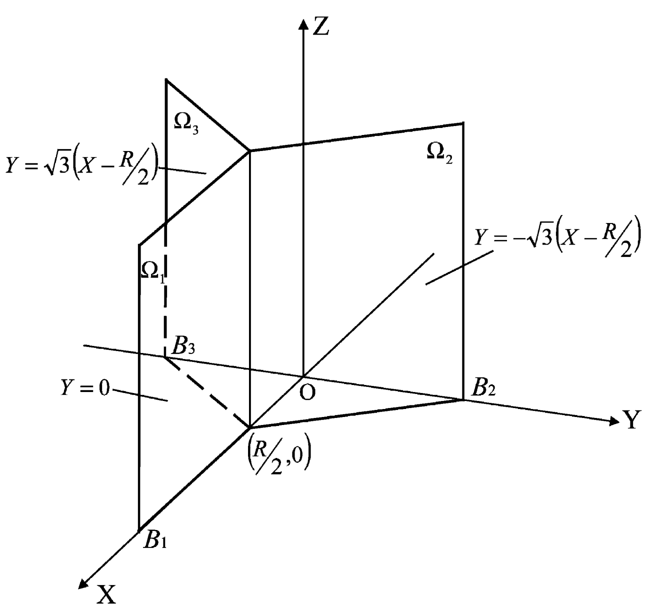

Fig. 3. Illustration of the three constraint planes.

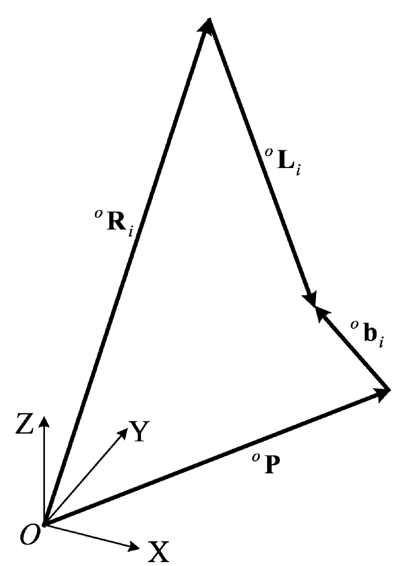

Fig. 4. Close loop of linkage i of the machine tool structure.

$$^{o}\mathbf{L}_i = {}^{o}\mathbf{b}_i + {}^{o}\mathbf{p} - {}^{o}\mathbf{R}_i = {}^{o}_{o_T}[R]\cdot{}^{o_T}\mathbf{b}_i + {}^{o}\mathbf{p} - {}^{o}\mathbf{R}_i \quad i = 1,2,3 \tag{16}$$

where the matrix ${}^{o}_{o_T}[R]$ describes the relative orientation of the spindle platform coordinate frame xyz to the base coordinate system XYZ, the left upper script o denotes the vector with respect to the base coordinate system XYZ, and the left under script o_T denotes the vector with respect to platform coordinate system xyz.

Since the position and the orientation of the spindle platform depend on the structural configuration of the machine tool, all these structural parameters will influence the positional accuracy of the spindle platform. In this section, the influences of different structure parameters on the position and orientation of the spindle platform are studied. An analytical method is proposed to investigate the sensitivity of different structure parameters to different positions and orientations of the platform.

For simplicity, all the scripts are omitted. Eq. (16) can thus be expressed by the following matrix form:

$$\begin{bmatrix} L_{iX} \\ L_{iY} \\ L_{iZ} \end{bmatrix} = \begin{bmatrix} k_1 & m_1 & n_1 \\ k_2 & m_2 & n_2 \\ k_3 & m_3 & n_3 \end{bmatrix} \cdot \begin{bmatrix} b_{ix} \\ b_{iy} \\ b_{iz} \end{bmatrix} + \begin{bmatrix} x_T \\ y_T \\ z_T \end{bmatrix} - \begin{bmatrix} R_{iX} \\ R_{iY} \\ R_{iZ} \end{bmatrix} \tag{17}$$

Rewrite Eq. (17) into three components as

$$L_{iX} = k_1 b_{ix} + m_1 b_{iy} + n_1 b_{iz} + x_T - R_{ix} = \cos\beta\cos\gamma b_{ix} - \cos\beta\sin\gamma b_{iy} + \sin\beta b_{iz} + x_T - R_{ix}$$

$$L_{iY} = k_2 b_{ix} + m_2 b_{iy} + n_2 b_{iz} + y_T - R_{iY} = (\sin\alpha\sin\beta\cos\gamma + \cos\alpha\sin\gamma) b_{ix} + (-\sin\alpha\sin\beta\sin\gamma + \cos\alpha\cos\gamma) b_{iy} - \sin\alpha\cos\beta b_{iz} + y_T - R_{iY}$$

$$L_{iZ} = k_3 b_{ix} + m_3 b_{iy} + n_3 b_{iz} + z_T - R_{iZ} = (-\cos\alpha\sin\beta\cos\gamma + \sin\alpha\sin\gamma) b_{ix} + (\cos\alpha\sin\beta\sin\gamma + \sin\alpha\cos\gamma) b_{iy} + \cos\alpha\cos\beta b_{iz} + z_T - R_{iZ}$$

Hence, the length of strut i can be calculated by

$$l_i^2 = \|\mathbf{L}_i\|^2 = L_{iX}^2 + L_{iY}^2 + L_{iZ}^2 \tag{18}$$

Introducing the following trigonometrical formulae

$$\sin\phi = \frac{2\tan(\phi/2)}{1 + \tan^2(\phi/2)};$$

$$\cos\phi = \frac{1 - \tan^2(\phi/2)}{1 + \tan^2(\phi/2)}$$

and letting the variables $a = \tan(\alpha/2)$, $b = \tan(\beta/2)$; $c = \tan(\gamma/2)$ we have

$$\sin\alpha = \frac{2a}{1 + a^2}; \quad \cos\alpha = \frac{1 - a^2}{1 + a^2}$$

$$\sin\beta = \frac{2b}{1 + b^2}; \quad \cos\beta = \frac{1 - b^2}{1 + b^2} \tag{19}$$

$$\sin\gamma = \frac{2c}{1 + c^2}; \quad \cos\gamma = \frac{1 - c^2}{1 + c^2}$$

According to the kinematics analysis described in the earlier session, those three degrees of freedom of the spindle platform are defined as one linear motion z_T in the Z direction and two angular motions, α and β, about the X- and Y-axes, respectively. In other words, parameters x_T, y_T, and γ are dependent on the orientation angles of the platform, as clearly seen in Eqs. (13) and (14). Now, substituting Eq. (14) and Eq. (19) into Eq. (18), a new algebraic equation can be obtained as follows:

$$F = F(z_T,a,b,c,R,r,b_{ix},b_{iy},b_{iz},R_{iX},R_{iY},R_{iZ},l_i) = A1^2 + A2^2 + A3^2 - (1 + a^2)^2(1 + b^2)^2(1 + c^2)^2 l_i^2 = 0 \tag{20}$$

where

$$A1 = (1 + a^2)(1 - b^2)(1 - c^2)\left(b_{ix} + \frac{r}{2}\right) - 2c(1 + a^2)(1 - b^2)b_{iy} + 4rabc - r\frac{(1 - a^2)(1 + b^2)(1 - c^2)}{2} + (1 + a^2)(1 + b^2)(1 + c^2)\left(\frac{R}{2} - R_{iX}\right)$$

$$A2 = [4ab(1 - c^2) + 2c(1 - a^2)(1 + b^2)](b_{ix} - r) + [(1 - a^2)(1 + b^2)(1 - c^2) - 8abc]b_{iy} - (1 + a^2)(1 + b^2)(1 + c^2)R_{iY}$$

$$A3 = [-2b(1 - a^2)(1 - c^2) + 4ac(1 + b^2)]b_{ix} + [4bc(1 - a^2) + 2a(1 + b^2)(1 - c^2)]b_{iy} + (1 - a^2)(1 - b^2)(1 + c^2)b_{iz} + (1 + a^2)(1 + b^2)(1 + c^2)(z_T - R_{iZ})$$

It is noted from Eq. (13) that the variable c in Eq. (20) is also a function of a and b. In addition, as shown in Fig. 2, the radius R of the outer circle passing through point R_i is a function of R_{iX} and R_{iY} (i = 1 to 3), and the radius r of the inner circle passing through joints b_i is a function of b_{ix} and b_{iy} (i = 1 to 3). Therefore, variables R and r in Eq. (20) can be expressed by

$$R = f(R_{iX},R_{iY}) = \left[\left(R_{iX} - \frac{1}{3}\sum_i^3 R_{iX}\right)^2 + \left(R_{iY} - \frac{1}{3}\sum_i^3 R_{iY}\right)^2\right]^{1/2}$$

$$r = f(b_{ix},b_{iy}) = \left[\left(b_{ix} - \frac{1}{3}\sum_i^3 b_{ix}\right)^2 + \left(b_{iy} - \frac{1}{3}\sum_i^3 b_{iy}\right)^2\right]^{1/2}$$

Eq. (20) shows that a complete kinematics model of the parallel mechanism composes of two sets of parameters, namely the structure parameters (l_i, b_{ix}, b_{iy}, b_{iz}, R_{ix}, R_{iy}, R_{iz}) and the platform's position parameters (z_T, α, β). The influences of the structure parameters on the position parameters reflect the structural sensitivity, or the positional sensitivity of the platform. This can be realized mathematically by the operation of partial differentiation as follows.

Differentiating Eq. (20) with respect to all structure parameters and position parameters for each structure loop yields

$$\delta F = A_i\delta T + B_i\delta P_i = 0 \quad i = 1,2,3 \tag{21}$$

where

$$A_i\delta T = \left(\frac{\partial F}{\partial \alpha}\right)_i \delta\alpha + \left(\frac{\partial F}{\partial \beta}\right)_i \delta\beta + \left(\frac{\partial F}{\partial Z_T}\right)_i \delta Z_T$$

$$B_i = \left[\frac{\partial F}{\partial R_{ix}}\ \frac{\partial F}{\partial R_{iy}}\ \frac{\partial F}{\partial R_{iz}}\ \frac{\partial F}{\partial b_{ix}}\ \frac{\partial F}{\partial b_{iy}}\ \frac{\partial F}{\partial b_{iz}}\ \frac{\partial F}{\partial l_i}\right] \in \Re^{1\times 7}$$

$$\delta P_i = [\delta R_{ix}\ \ \delta R_{iy}\ \ \delta R_{iz}\ \ \delta b_{ix}\ \ \delta b_{iy}\ \ \delta b_{iz}\ \ \delta l_i]^T \in \Re^{7\times 1}$$

Integrating the three loops of Eq. (21) together and separating the position parameters and structure parameters to different sides yields the following simplified matrix form

$$-A\delta T = B\delta P \tag{22}$$

where

$$A = \begin{bmatrix} \left(\frac{\partial F}{\partial \alpha}\right)_1 & \left(\frac{\partial F}{\partial \beta}\right)_1 & \left(\frac{\partial F}{\partial Z_T}\right)_1 \\ \left(\frac{\partial F}{\partial \alpha}\right)_2 & \left(\frac{\partial F}{\partial \beta}\right)_2 & \left(\frac{\partial F}{\partial Z_T}\right)_2 \\ \left(\frac{\partial F}{\partial \alpha}\right)_3 & \left(\frac{\partial F}{\partial \beta}\right)_3 & \left(\frac{\partial F}{\partial Z_T}\right)_3 \end{bmatrix} \in \Re^{3\times 3}$$

$$B = \begin{bmatrix} B_1 & 0 & 0 \\ 0 & B_2 & 0 \\ 0 & 0 & B_3 \end{bmatrix} \in \Re^{3\times 21}$$

$$\delta P = [\delta P_1\ \ \delta P_2\ \ \delta P_3]^T \in \Re^{21\times 1}$$

Then

$$\delta T = (-A^{-1}) * B\delta P$$

Let

$$C = ((-A)^{-1} * B) \in \Re^{3\times 21} \tag{23}$$

Matrix C represents the sensitivity matrix of position parameters with respect to the structural parameters with the coupling effect of three independent structure loops. The differential terms are

$$\frac{\partial F}{\partial a} = 2A1\frac{\partial A1}{\partial a} + 2A2\frac{\partial A2}{\partial a} + 2A3\frac{\partial A3}{\partial a} - 4a(1 + a^2)$$

$$(1 + b^2)^2(1 + c^2)^2 l_i^2$$

$$\frac{\partial F}{\partial b} = 2A1\frac{\partial A1}{\partial b} + 2A2\frac{\partial A2}{\partial b} + 2A3\frac{\partial A3}{\partial b} - 4b(1 + a^2)^2$$

$$(1 + b^2)(1 + c^2)^2 l_i^2$$

$$\frac{\partial F}{\partial c} = 2A1\frac{\partial A1}{\partial c} + 2A2\frac{\partial A2}{\partial c} + 2A3\frac{\partial A3}{\partial c} - 4c(1 + a^2)^2$$

$$(1 + b^2)^2(1 + c^2) l_i^2$$

$$\frac{\partial F}{\partial R_{ix}} = \frac{\partial F}{\partial R}\frac{\partial R}{\partial R_{ix}} + \frac{\partial F}{\partial A1}\frac{\partial A1}{\partial R_{ix}}$$

$$\frac{\partial F}{\partial R_{iy}} = \frac{\partial F}{\partial R}\frac{\partial R}{\partial R_{iy}} + \frac{\partial F}{\partial A2}\frac{\partial A2}{\partial R_{iy}}$$

$$\frac{\partial F}{\partial R_{iz}} = \frac{\partial F}{\partial A3}\frac{\partial A3}{\partial R_{iz}}$$

$$\frac{\partial F}{\partial b_{ix}} = \frac{\partial F}{\partial r}\frac{\partial r}{\partial b_{ix}} + \frac{\partial F}{\partial A1}\frac{\partial A1}{\partial b_{ix}} + \frac{\partial F}{\partial A2}\frac{\partial A2}{\partial b_{ix}} + \frac{\partial F}{\partial A3}\frac{\partial A3}{\partial b_{ix}}$$

$$\frac{\partial F}{\partial b_{iy}} = \frac{\partial F}{\partial r}\frac{\partial r}{\partial b_{iy}} + \frac{\partial F}{\partial A1}\frac{\partial A1}{\partial b_{iy}} + \frac{\partial F}{\partial A2}\frac{\partial A2}{\partial b_{iy}} + \frac{\partial F}{\partial A3}\frac{\partial A3}{\partial b_{iy}}$$

$$\frac{\partial F}{\partial b_{iz}} = 2A3 \times (1-a^2)(1-b^2)(1-c^2)$$

$$\frac{\partial F}{\partial l_i} = -2l_i \times (1 + a^2)^2(1 + b^2)^2(1 + c^2)^2$$

$$\frac{\partial c}{\partial a} = -b$$

$$\frac{\partial c}{\partial b} = -a$$

5. Examples and discussions

Based on the sensitivity matrix of Eq. (23), simulated examples are given in terms of different platform poses (α and β = 0°, 5°, 10°, 15°, 20°, 25°). The calculation is performed according to the obtained data of the prototype machine tool from experiments as: (R = 349.368 mm, r = 199.950 mm, l_1 = 1107.592 mm, l_2 = 1107.664 mm, l_3 = 1107.526 mm). The results are listed in Tables 1–3. It is seen that when the platform pose is at α=β=0, the parallel structure is symmetric so that the difference in sensitivity values between three structure branches is slight. The sensitivities of all position parameters with respect to specific structure parameter at different platform poses are summarized in the following.

1. With spindle platform pose $\alpha = \beta = 0$, because the structure branch #1 coincides with the X-axis, the sensitivities of all the parameters (R_{1x} R_{1y} R_{1z} b_{1x} b_{1y} b_{1z} l_1) have no influence on the orientation parameter of α.

Table 1
Sensitivity analysis of the position z_T (z_T = 300 mm)

	$\alpha = 0, \beta = 0$	$\alpha = 5, \beta = 5$	$\alpha = 10, \beta = 10$	$\alpha = 15, \beta = 15$	$\alpha = 20, \beta = 20$	$\alpha = 25, \beta = 25$
$\partial z_T/\partial R_{1x}$	0.0302	0.0210	0.0118	0.0023	−0.0077	−0.0180
$\partial z_T/\partial R_{1y}$	0.0000	0.0000	0.0000	0.0000	0.0000	0.0000
$\partial z_T/\partial R_{1z}$	0.3333	0.2311	0.1282	0.0244	−0.0783	−0.1744
$\partial z_T/\partial b_{1x}$	−0.0453	−0.0112	0.0048	0.0030	−0.0160	−0.0495
$\partial z_T/\partial b_{1y}$	0.0000	−0.0202	−0.0222	−0.0062	0.0258	0.0692
$\partial z_T/\partial b_{1z}$	−0.3333	−0.2294	−0.1243	−0.0228	0.0691	0.1433
$\partial z_T/\partial l_1$	−0.3364	−0.2326	−0.1288	−0.0245	0.0786	0.1753
$\partial z_T/\partial R_{2x}$	−0.0264	−0.0384	−0.0525	−0.0699	−0.0910	−0.1159
$\partial z_T/\partial R_{2y}$	0.0457	0.0665	0.0910	0.1210	0.1577	0.2008
$\partial z_T/\partial R_{2z}$	0.3333	0.4747	0.6199	0.7680	0.9163	1.0581
$\partial z_T/\partial b_{2x}$	0.0226	0.0738	0.1504	0.2519	0.3760	0.5166
$\partial z_T/\partial b_{2y}$	−0.0392	−0.0977	−0.1815	−0.2883	−0.4132	−0.5462
$\partial z_T/\partial b_{2z}$	−0.3333	−0.4711	−0.6012	−0.7166	−0.8092	−0.8693
$\partial z_T/\partial l_2$	−0.3364	−0.4819	−0.6344	−0.7939	−0.9589	−1.1231
$\partial z_T/\partial R_{3x}$	−0.0264	–0.0232	–0.0197	−0.0159	−0.0121	−0.0084
$\partial z_T/\partial R_{3y}$	−0.0457	−0.0402	−0.0341	−0.0276	−0.0210	−0.0145
$\partial z_T/\partial R_{3z}$	0.3333	0.2941	0.2519	0.2076	0.1619	0.1163
$\partial z_T/\partial b_{3x}$	0.0226	0.0456	0.0609	0.0679	0.0665	0.0571
$\partial z_T/\partial b_{3y}$	0.0392	0.0089	−0.0138	−0.0281	−0.0338	−0.0317
$\partial z_T/\partial b_{3z}$	−0.3333	−0.2919	−0.2443	−0.1937	−0.1430	−0.0955
$\partial z_T/\partial l_3$	−0.3364	−0.2966	−0.2543	−0.2100	−0.1643	−0.1184

Table 2
Sensitivity analysis of the orientation angular α (z_T = 300 mm)

	$\alpha = 0, \beta = 0$	$\alpha = 5, \beta = 5$	$\alpha = 10, \beta = 10$	$\alpha = 15, \beta = 15$	$\alpha = 20, \beta = 20$	$\alpha = 25, \beta = 25$
$\partial\alpha/\partial R_{1x}$	0.0000	0.0000	0.0000	0.0000	0.0000	–0.0001
$\partial\alpha/\partial R_{1y}$	0.0000	0.0000	0.0000	0.0000	0.0000	0.0000
$\partial\alpha/\partial R_{1z}$	0.0000	–0.0001	–0.0002	–0.0003	–0.0005	–0.0007
$\partial\alpha/\partial b_{1x}$	0.0000	0.0000	0.0000	0.0000	–0.0001	–0.0002
$\partial\alpha/\partial b_{1y}$	0.0000	0.0000	0.0000	0.0001	0.0002	0.0003
$\partial\alpha/\partial b_{1z}$	0.0000	0.0001	0.0002	0.0003	0.0004	0.0006
$\partial\alpha/\partial l_1$	0.0000	0.0001	0.0002	0.0003	0.0005	0.0007
$\partial\alpha/\partial R_{2x}$	–0.0002	–0.0002	–0.0003	–0.0003	–0.0004	–0.0004
$\partial\alpha/\partial R_{2y}$	0.0004	0.0004	0.0005	0.0005	0.0006	0.0008
$\partial\alpha/\partial R_{2z}$	0.0029	0.0030	0.0031	0.0033	0.0036	0.0040
$\partial\alpha/\partial b_{2x}$	0.0002	0.0005	0.0008	0.0011	0.0015	0.0020
$\partial\alpha/\partial b_{2y}$	–0.0003	–0.0006	–0.0009	–0.0013	–0.0016	–0.0021
$\partial\alpha/\partial b_{2z}$	–0.0029	–0.0029	–0.0030	–0.0031	–0.0032	–0.0033
$\partial\alpha/\partial l_2$	–0.0029	–0.0030	–0.0032	–0.0035	–0.0038	–0.0043
$\partial\alpha/\partial R_{3x}$	0.0002	0.0002	0.0002	0.0002	0.0002	0.0002
$\partial\alpha/\partial R_{3y}$	0.0004	0.0004	0.0004	0.0004	0.0004	0.0004
$\partial\alpha/\partial R_{3z}$	–0.0029	–0.0029	–0.0030	–0.0030	–0.0031	–0.0033
$\partial\alpha/\partial b_{3x}$	–0.0002	–0.0005	–0.0007	–0.0010	–0.0013	–0.0016
$\partial\alpha/\partial b_{3y}$	–0.0003	–0.0001	0.0002	0.0004	0.0007	0.0009
$\partial\alpha/\partial b_{3z}$	0.0029	0.0029	0.0029	0.0028	0.0028	0.0027
$\partial\alpha/\partial l_3$	0.0029	0.0029	0.0030	0.0031	0.0032	0.0033

2. The sensitivity values of all structure parameters to displacement parameter (z_T) are larger than the orientation parameters (α, β). It is because the unit of angle is in degree and the unit of displacement is in mm.

3. With the spindle platform pose $\alpha = \beta = 0$, branches #2 and #3 are symmetric in the coordinate system, so the sensitivities are equal in magnitude but could be different in the sign.

4. Table 1 shows that the sensitivities of the parameters R_{iX}, R_{iY}, b_{ix}, b_{iy} and b_{iz} (i = 1 to 3) influencing the position z_T of the spindle platform are varied with the platform's angles α and β in different cases of 0°, 15° and 25°. For example, the sensitivity of the parameter R_{iX} varies from 0.0302 at the pose ($\alpha = \beta = 0^0$) to −0.018 at the pose ($\alpha = \beta = 25^0$). Compared to R_{iZ}, the sensitivities of the parameters R_{iX} and R_{iY} to z_T are

Table 3
Sensitivity analysis of the orientation angular β (z_T = 300 mm)

	$\alpha=0$, $\beta=0$	$\alpha=5$, $\beta=5$	$\alpha=10$, $\beta=10$	$\alpha=15$, $\beta=15$	$\alpha=20$, $\beta=20$	$\alpha=25$, $\beta=25$
$\partial\beta/\partial R_{1x}$	–0.0003	–0.0003	–0.0003	–0.0003	–0.0003	–0.0003
$\partial\beta/\partial R_{1y}$	0.0000	0.0000	0.0000	0.0000	0.0000	0.0000
$\partial\beta/\partial R_{1z}$	–0.0033	–0.0033	–0.0033	–0.0033	–0.0033	–0.0032
$\partial\beta/\partial b_{1x}$	0.0005	0.0002	–0.0001	–0.0004	–0.0007	–0.0009
$\partial\beta/\partial b_{1y}$	0.0000	0.0003	0.0006	0.0008	0.0011	0.0013
$\partial\beta/\partial b_{1z}$	0.0033	0.0033	0.0032	0.0031	0.0029	0.0026
$\partial\beta/\partial l_1$	0.0034	0.0033	0.0033	0.0033	0.0033	0.0032
$\partial\beta/\partial R_{2x}$	–0.0001	–0.0001	–0.0001	–0.0002	–0.0002	–0.0002
$\partial\beta/\partial R_{2y}$	0.0002	0.0002	0.0002	0.0003	0.0003	0.0003
$\partial\beta/\partial R_{2z}$	0.0017	0.0017	0.0017	0.0017	0.0017	0.0016
$\partial\beta/\partial b_{2x}$	0.0001	0.0003	0.0004	0.0006	0.0007	0.0008
$\partial\beta/\partial b_{2y}$	–0.0002	–0.0003	–0.0005	–0.0006	–0.0008	–0.0008
$\partial\beta/\partial b_{2z}$	–0.0017	–0.0017	–0.0016	–0.0016	–0.0015	–0.0013
$\partial\beta/\partial l_2$	–0.0017	–0.0017	–0.0017	–0.0018	–0.0018	–0.0017
$\partial\beta/\partial R_{3x}$	–0.0001	–0.0001	–0.0001	–0.0001	–0.0001	–0.0001
$\partial\beta/\partial R_{3y}$	–0.0002	–0.0002	–0.0002	–0.0002	–0.0002	–0.0002
$\partial\beta/\partial R_{3z}$	0.0017	0.0016	0.0016	0.0016	0.0016	0.0016
$\partial\beta/\partial b_{3x}$	0.0001	0.0003	0.0004	0.0005	0.0006	0.0008
$\partial\beta/\partial b_{3y}$	0.0002	0.0000	–0.0001	–0.0002	–0.0003	–0.0004
$\partial\beta/\partial b_{3z}$	–0.0017	–0.0016	–0.0015	–0.0015	–0.0014	–0.0013
$\partial\beta/\partial l_3$	–0.0017	–0.0016	–0.0016	–0.0016	–0.0016	–0.0016

significantly less. Similarly, the sensitivities of the parameters b_{ix} and b_{iy} influencing the position z_T are also less than b_{iz} (h). It means the cutter's height position is more sensitive to the height related joint parameters.

5. Tables 2 and 3 show that the sensitivities of all the parameters R_{iX}, R_{iY}, R_{iZ}, b_{ix}, b_{iy} and b_{iz} (i = 1 to 3) influencing the orientation of the spindle platform are also varied with the platform's angles α and β in different cases of 0°, 15° and 25°. Obviously, the Z-coordinate parameters also have larger influence on the orientation angles of the spindle platform, compared to the X- and Y-coordinate parameters. In other words, the positioning accuracy of the sliders (R_{iZ}) and b_{iz} are more important to the accuracy of the orientation angles of the spindle platform.

6. The data in Tables 1–3 clearly show that parameter l_i (i = 1 to 3) have larger influence on the platform position z_T and orientation angles α and β and at different platform's poses. Therefore, the nominal strut length (l_i) is a very sensitive parameter to the accuracy of the cutter position z_T as well as the platform's angles.

7. As α and β increase the platform is tilted to the loop 2 direction. The sensitivity of this loop's structure parameters is more significant.

8. The computational results are consistent with the physical phenomenon of the machine tool. The sensitivity investigation of the position and the orientation of the spindle platform in the workspace can also be calculated by using Eq. (23), while the platform's angles α and β are either assigned positive or negative.

6. Conclusions

Inverse kinematics model of the parallel mechanism has been derived to compute the positions of the rotational joints R_i and the ball joints b_i (i = 1 to 3) at given values of α, β and z_T. The sensitivity analysis of the accuracy of the cutter location with respect to some structure parameters is also proposed in this study. From simulated examples it shows that the sensitivity of structure parameters will change as the platform varies its orientations. Among all parameters, the Z-coordinate parameters have larger influence on the position and the orientation of the spindle platform in different poses. The sensitivity analyses of platform's position with respect to the structure parameters have demonstrated that the positioning accuracy of the parallel sliders, the original strut length, and the tool length are the most sensitive parameters influencing the position and orientation of the spindle platform, or the cutter location, in practice.

References

[1] J. Wang, O. Masory, On the accuracy of a Stewart platform—Part I: The effect of manufacturing tolerances, in: Proc. of IEEE Int. Conf. on Robotics and Automation, Atlanta, USA, 2–6 May, 1993, pp.114–120.

[2] D. Kim, W. Chung, Y. Youm, Singularity analysis of 6-DOF manipulators with the analytical representation of the determinant, in: Proc. of IEEE Int. Conf. on Robotics and Automation, Michigan, USA, 10–15 May, 1999, pp.889–894.

[3] C. Park, Computational aspect of manipulators via product of exponential formula for robot kinematics, IEEE Trans. Automatic Control 39 (9) (1994) 643–647.

[4] J. Song, J. Mou, C. King, Kinematic performance analysis of a parallel chain hexapod machine, in: Proc. of ASME IMECE Symposium on Recent Advances in Machine Tools and Metrology, ASME IMECE, MED-Vol. 8, 1998, pp. 673–680.

[5] G.L. Yang, I.M. Chen, W.K. Lim, S.H. Yeo, Design and kinematic analysis of modular reconfigurable parallel robots, in: Proc. of IEEE Int. Conf. on Robotics and Automation, Michigan, USA, 10–15 May, 1999, pp. 2501–2506.

[6] X.J. Liu, J.S. Wang, F. Gao, L.P. Wang, On the analysis of a new spatial three-degree-of freedom parallel manipulator, IEEE Trans. Robotics Automation 17 (6) (2001) 959–968.

[7] G.L. Yang, I.M. Chen, W.K. Lim, S.H. Yeo, Self-calibration of three-legged modular reconfigurable parallel robots based on leg-end distance error, Robotica 19 (1999) 187–198.

[8] R. Nair, J.H. Maddocks, On the forward kinematics of parallel manipulators, Int. J. Robotics Res. 13 (2) (1994) 171–188.

[9] R.P. Podhorodeski, K.H. Pittens, A class of parallel manipulators based on kinematically simple branches, Trans ASME J. Mech. Design 116 (5) (1994) 908–914.

[10] T. Ropponen, T. Arai, Accuracy analysis of a modified Stewart platform manipulator, in: Proc. of IEEE Int. Conf. on Robotics and Automation, Nagoya, Japan, 21–27 May, 1995, pp. 521–525.

[11] O. Masory, J. Wang, H. Zhuang, On the accuracy of a Stewart platform–Part II: kinematic calibration and compensation, in: Proc. of IEEE Int. Conf. on Robotics and Automation, Atlanta, USA, 2–6 May, 1993, pp. 725–731.

[12] S.H. Chen, T.H. Chang, M.H. Hsei, Analytical modelling of manufacturing errors on the accuracy for TRR-XY hybrid parallel link machine tool, IMechE Part B, J. Eng. Manufacture 215 (2001) 1203–1216.

[13] T.H. Chang, S.L. Chen, C.A. Kang, I. Inasaki, Design optimization of the linkage dimension for a hybrid-type parallel kinematics machine tool, IMechE part K, J. Multibody Dyn. 216 (2002) 143–156.

[14] J.W. Zhao, K.C. Fan, T.H. Chang, Z. Li, Error analysis of a serial-parallel type machine tool, J. Adv. Manufact. Technol. 19 (2002) 174–179.